# An analysis of Chosen Image Formation Algorithms for Synthetic Aperture Radar with FMCW

Marta Okoń-Fąfara, Piotr Serafin, and Adam Kawalec

*Abstract*—**The modelling of FMCW SAR systems, due to long signal duration time, commonly used start-stop approximation for pulsed radars causes errors in the image. Continuous motion of the radar platform results in additional range-azimuth couplings and range walk term that should be considered in processing of signal from this type of radar. The paper presents an analysis of the following algorithms: Time Domain Correlation (TDC), Range Doppler Algorithm (RDA), and Range Migration Algorithm (RMA). The comparison of the algorithms is based on theoretical estimation of their computation complexity and the quality of images obtained on the basis of real signals of FMCW SAR systems.**

*Keywords*—**signal processing, synthetic aperture radar, Time Domain Correlation, Range Doppler Algorithm, Range Migration Algorithm**

## I. INTRODUCTION

IN the field of aerial observations, sensors of possible small dimensions, low cost, while ensuring high resolution of the obtained images are becoming more and more popular [1]. Their potential applications include field mapping, environment observation (observation of forest cover or water surface to detect pollutions), monitoring of construction sites, and various military applications [2]. Because such sensors are usually installed onboard of Unmanned Aerial Vehicles (UAVs), they have to be possibly small, light, and consume little energy. Additionally, the application of radar sensors allows for observation of relatively large terrain surface independently of the weather conditions and the time of day. Unfortunately, in typical configuration they have low azimuth resolution. This drawback can be removed using Synthetic Aperture Radar (SAR) systems which allow to achieve high resolution images. Most often they operate as coherent pulse radars with carefully designed intrapulse structure. Usually there are used Linear Frequency Modulation (LFM) waveforms. The low level of sidelobes in the time domain, after the matched filtering is ensured by application of Non-Linear Frequency Modulation (NLFM) waveforms. There are considered also signals with more complex time-frequency intrapulse structure. Their synthesis, however, requires more sophisticated processing [3,4]. Where limited radar sensor's dimensions,

weight and cost are desirable, Frequency Modulated Continuous Wave (FMCW) [1] SAR system, are applied.

For pulsed radar SAR systems modeling, the "start-stop" approximation is commonly used. Due to the relatively short pulse duration it assumes that the platform is stationary during the pulse transmission process. Thus, the difference in echo delays from a given object results only from the change of the radar position. The radar movement induces changes in the distance between the radar and the object (so-called Range Migration (RM)). However, FMCW SAR systems employ long waveforms that allow us to obtain larger radar range [5], while keeping the peak pulse power at a low level. The breaks between the transmitted pulses are short enough to assume the transmission continuity. As a result, the previously accepted approximation ceases to be valid and taking the movement of radar platform into account is necessary. In the FMCW radar signal processing additional couplings between range and azimuth components that result from the Doppler effect should be considered [6,7]. Thus, the application of typical algorithms of SAR image synthesis without adequate modifications will lead to image distortions.

Most often the algorithms of SAR image synthesis are divided with respect to the field of processing, distinguishing the algorithms operating in the time or frequency domains. The first group comprises the Time Domain Correlation – TDC algorithm, in which the image is formulated through the matched filtering along a synthetic aperture i.e. through the convolution of the raw signal with so-called reference function. The second group includes the Range Doppler Algorithm (RDA) that synthesizes image through the multiplication of the reference function spectrum with the raw SAR signal spectrum. The last of the discussed algorithms is the Range Migration Algorithm (RMA) known also in the literature as the Omega-k algorithm [8]. It ensures precise processing of data, even for long apertures and large squint angles of the radar. It realizes the operation called the Stolt interpolation that synthesizes image by reconstruction of the electromagnetic wave front.

Many other algorithms of FMCW SAR image synthesis, including modifications of the above mentioned, are described in the literature and usually a comparison of the effects of their performance is presented. These descriptions are focused, first of all, on quality of a point objects synthesis, including the width of the mainlobe and the level of sidelobes (e.g. [9, 10]). There is little quantitative estimations of computational complexity of those algorithms [e.g. 11] available. This paper presents the comparison, taking into account both criteria, in relation to the implemented algorithms and SAR images obtained from experimental investigations.

## II. MODEL OF FMCW SIGNAL

The SAR data processing is based on the two-dimensional, spatially dependent correlation of the raw echo signal with the echo of a point object [9]. If the transmitted FMCW signal $s_t(t)$ has the form [10]

$$s_t(t) = \text{rect}\left(\frac{t - T/2}{T}\right) \cos\left(2\pi f_{\min} t + \frac{\mu t^2}{2}\right) \quad (1)$$

where: $T$ - is the duration of reference signal, $f_{\min}$ - is the signal's minimum frequency, $B$ - is the bandwidth of the signal's frequency changes, $\mu$ - is the of LFM CW changes

$$\mu = \frac{2\pi B}{T} \quad (2)$$

then the signal of the point object's echo can be written as [10]

$$s_r(t) = \text{rect}\left(\frac{t - \tau - T/2}{T}\right) \times$$
$$\times \cos\left[2\pi f_{\min}(t - \tau) + \frac{\mu(t - \tau)^2}{2}\right] \quad (3)$$

where $\tau$ - is the echo signal delay due to the radar-object distance.

To simplify the considerations, an initial phase of the sounding signal as equal to zero and for all signals a unit amplitude is assumed. Instantaneous frequencies of the sounding signal and the echo signal are given in Fig. 1.
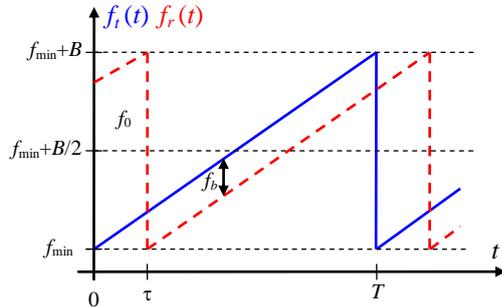


Fig. 1. Instantaneous frequencies of the sounding signal and the echo signal [10].

After the multiplication of the echo signal (3) with the direct and $\pi/2$-shifted transmitted signal, the complex down-converted signal of a beat frequency is expressed as [10]

$$s_b(t) = \text{rect}\left(\frac{t - T/2 - \tau/2}{T - \tau}\right) \times$$
$$\times \exp\left\{j\left[\mu\tau t + 2\pi f_{\min}\tau - \frac{\mu\tau^2}{2}\right]\right\} \quad (4)$$

When a radar sensor approaches a stationary point object on the Earth surface with the radial velocity $v_{RR}$ the echo signal's delay is determined as

$$\tau = \frac{2}{c}(R_0 - v_{RR}t) = \tau_0 - \frac{2v_{RR}}{c}t \quad (5)$$

where: $R_0$ - is the initial radar –object distance, $c$ - is the electromagnetic wave propagation velocity, $v_{RR}$ - is the radar-object mutual velocity (radial velocity), $\tau_0$ - is the initial, i.e. at

the beginning of the LFM ramp, signal delay from the object at $R_0$ distance.

Because the radar sensor moves with the linear velocity $v_R$, both the echo signal delay $\tau_0$ as well as the mutual (radial) velocity $v_{RR}$ change in time.

Each of the described algorithms operates on the range-compressed signal. The range compression of the FMCW signal is in fact its Fourier transform and the range-compressed signal can be expressed as [10]

$$S_b(f,u) = \exp\left\{j2\pi\left[f_0\tau_0(u) - f_0\frac{v_{RR}(u)}{c}T + \frac{B}{2}\tau_0(u)\right]\right\} \times$$
$$\times\left[T - \tau_0(u)\right]\text{sinc}\left[2\pi\left(f - \frac{B}{T}\tau_0(u) + f_0\frac{2v_{RR}(u)}{c}\right)\frac{T - \tau_0(u)}{2}\right]. \quad (6)$$

This signal should be sampled in the fast time with the period $t_s$ and in the slow time with Pulse Repetition Interval (PRI). During the development phase of the SAR system the PRI must be chosen with respect to the Nyquist criterion in the spatial domain. This is strictly connected with the platform velocity, the wavelength used and the width of the main lobe of the antenna system. If the criterion is not satisfied, the aliasing phenomenon occurs and false objects appear in the image [12].

The above function describes the range-compressed point object echo signal. In the SAR processing, each point of an image is regarded as a potential source of the echo signal. Thus, the echo signal delay $\tau_0$ becomes dependent also on range (i.e., on the number of the range cell $k$). Additionally, the azimuth coordinates become related to the center of the synthetic aperture.

## III. THE TDC ALGORITHM

The TDC algorithm consists of the definitional convolution of the raw signal with the reference point object echo. In practice, it means a summation of the signal along synthetic aperture with the phase correction term which responds to the difference of the signal path due to the changing radar position. This operation can be described with the following equation [10]

$$G(m,k) = \sum_{b=-N_a/2}^{N_a/2} S\left[m + b, k_0(m)\right] w_{ref}(k,b) \quad (7)$$

where:

$b$    is the number of the synthetic aperture element that changes in the range $\langle -N_a/2, N_a/2 \rangle$,

$k_0(k,b)$ determines the range migration of the signal

$$k_0(k,b) = \frac{N}{2\pi}t_s\left(\mu\tau_0(k,b) - 2\pi f_{\min}\frac{2v_{RR}(k,b)}{c}\right) \quad (8)$$

In equation (8) $w_{ref}(k,b)$ is the reference function describing the changes of the initial phase of the echo signal after the range-compression [10]

$$w_{ref}(k,b) = \exp\left\{-j\left[\begin{array}{l} 2\pi f_{\min}\tau_0(k,b) - \dfrac{\mu\tau_0^2(k,b)}{2} + \\[2mm] + \left(\left(\mu\tau_0(k,b) - 2\pi f_{\min}\dfrac{2v_{RR}(k,b)}{c}\right)t_s - \dfrac{2\pi}{N}k\right)\dfrac{(L+l_0(k,b)-1)}{2} \end{array}\right]\right\}, \tag{9}$$

where:

$\tau_0(k,b)$ is the echo signal delay before the DFT determined in the following way

$$\tau_0(k,b) = \frac{2R(k,b)}{c} = $$
$$\frac{2\sqrt{R_0^2(k) + \delta y(b)}}{c} = $$
$$\frac{2\sqrt{(kdR + R_{\min})^2 + b^2 d^2}}{c} \tag{10}$$

$l_0(k,b)$ - is the echo signal delay before the azimuth compression and it is computed as,

$$l_0(k,b) = \left\lfloor \frac{\tau_0(k,b)}{t_s} \right\rfloor \tag{11}$$

$v_{RR}(k,b)$ - is the radial velocity of the object in respect to the radar, that is, the velocity of the radar's platform $v_R$, projected on the radar-object line,

$dR$ - is the size of a range cell after the DFT,

$d$ - is the distance between consecutive points along the radar trajectory.

The TDC algorithm has a high computational complexity of the $O(MNN_a)$ order, which is too high for many applications. However, due to the definitional forming of the reference function, it gives a basis for measuring the image quality of the other reconstruction algorithms [5].

## IV. THE RDA

In many applications SAR images are synthesized using the RDA which makes azimuth compression through the fast convolution of the raw signal and the reference function [13]. It means that the range-compressed radar's signal must be subjected to the Fourier transform in the azimuth direction, i.e., transferred into the range-Doppler – domain and then multiplied with the reference signal spectrum [1].
Azimuth spectra of the objects' echoes are centered around the zero frequency (Fig. 2). Their shape on the R-D plane is a hyperbole that reflects the function of radar-object distance changes (so called the range migration curve). The beat frequency of the down-converted signal in the FMCW system that is proportional to the distance may be expressed as a function of azimuth position as follows [13]

$$f_R(u) = \mu\frac{2R(u)}{c} \tag{12}$$

In the R-D domain it can be written as [13]

$$R(f_D) = \frac{R_0}{\sqrt{1 - \dfrac{\lambda^2 f_D^2}{4v_R^2}}} \tag{13}$$

where $R_0$ is the slant range, $\lambda$ is the length of the used carrier wave, $f_D$ is the current Doppler frequency.

Accordingly, the relationship between a differential frequency and azimuth (Doppler) frequency can be described as follows

$$f(f_D) = \frac{2\mu R_0}{c\sqrt{1 - \dfrac{\lambda^2 f_D^2}{4v_R^2}}} \tag{14}$$

To perform the matched filtering in the frequency domain properly, the echo signals of a single stationary point should be placed along the straight line. The straightening of the range migration curve is called the Range Cell Migration Correction – RCMC and it should be performed for each range. Thus, it is necessary to know a shape of the $f(f_D)$ relation.

The function (13) has been derived for a pulse radar, where the Doppler shift of the echo signal does not influence significantly on the target position along the image's range axis. In FMCW radars, the distance to the target is determined on the basis of the beat frequency, and the Doppler shift can disturb this value. In this case the range migration function takes the following form [13]

$$f(f_D) = f_D + \frac{2\mu R_0}{c\sqrt{1 - \dfrac{\lambda^2 f_D^2}{4v_R^2}}} \tag{15}$$

After RCMC, the corrected signal undergoes matched filtering by azimuth reference function, corresponding to the phase changes of the point target's echo signal along the synthetic aperture. For the slant range $R_0$ and determined length of the synthetic aperture $N_a$, the reference function takes the form [13]

$$w_{ref}(R_0) = $$
$$= FFT_a\left\{\exp\left[j2\pi\left(\frac{2\sqrt{R_0^2 + b^2}}{\lambda} + f_D\frac{2\sqrt{R_0^2 + b^2}}{c}\right)\right]\right\} \tag{16}$$

where $FFT_a\{\ \}$ is the fast Fourier transform along the azimuth, and $b$ - is the number of the synthetic aperture's element changing in the range $\langle -N_a/2, N_a/2\rangle$.
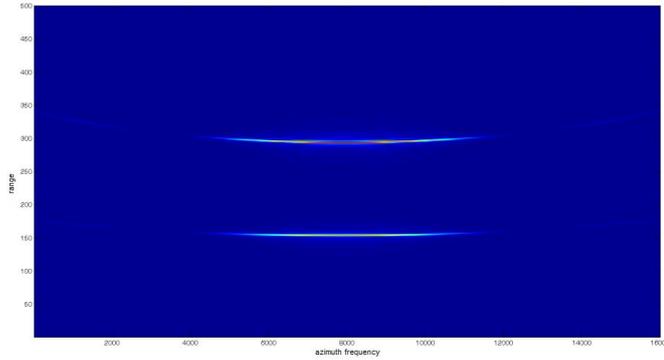
Fig. 2. The azimuth spectrum of the simulated signal [13]

Thus, the image synthesis of the range-compressed signal by RDA can be divided into two basic steps: the range cell migration correction and the azimuth compression [14].

Due to the application of the fast signal convolution, the matched filtering lasts significantly shorter than in case of the TDC algorithm. However, the quality of the obtained images depends on the number of the used reference functions because for each range bin it has different form. In order to simplify the calculations it is possible to assume range intervals in which the reference function does not change. This would speed up the algorithm, however induces some approximation errors within these intervals.

## V. THE RMA

The Range Migration Algorithm belongs to the group of the algorithms operating in wavenumber domain ($\omega - k$). It performs so called Stolt interpolation which formulates image through the reconstruction of an electromagnetic wave front [8]. In order to make the image synthesis from the range-compressed signal using RMA, the Fourier transform along the azimuth dimension should be firstly performed. The result takes the following form [14]

$$S(\omega, \omega_D) =$$
$$= P(\omega) \sum_n \exp\left( -j \sqrt{4 \frac{\omega^2}{c^2} - \frac{\omega_D^2}{V^2}} \, x_n - j \frac{\omega_D}{V} y_n \right),$$
$$= P(\omega) \sum_n \exp\left( -j \sqrt{4k^2 - k_u^2} \, x_n - j k_u y_n \right) \quad (17)$$

where $x$ - is the distance between the object and the radar, $y$ - is the direction of the radar movement, $P(\omega)$ - is the spectrum of the transmitted signal, $\omega_D$ is the Doppler pulsation in reference to radar position $u$ and taking $k_u = \omega_D / V$ as wavenumber in the Doppler frequency domain.

Subsequently, the matched filtering along the azimuth should be made. Due to the broadside configuration of the radar with zero squint angle, a simplified filter can be used [14]

$$h_{az}(m) = \exp\left[ j\pi\beta \left( m \cdot PRI \right)^2 \right], \quad (18)$$

where $PRI = 1/f_{PRF}$ is the pulse repetition interval, $m$ determines the number of the sample along the radar synthetic aperture $N_a$ (expressed in samples) and $\beta$ means the azimuth LFM rate expressed as [14]

$$\beta = -\frac{2V^2}{\lambda X_0}, \quad (19)$$

where $X_0$ - is the reference point range (usually the image center).

After the preliminary compression, the differential azimuth compression (DAC) should be done which will correct the phase of the signal in reference to the center of the image. The compressed signal $s_c(x, k_y)$ should be multiplied with the FMCW range-Doppler coupling signal phase corrector, that also includes the range migration correction according to the relation [15]

$$s_c'(x, k_y) = s_c(x, k_y) \exp\left( -j\pi c \frac{f_y^2}{4v^2 f_0} \Delta x_n \right), \quad (20)$$

where $f_y$ is the azimuth frequency, $f_0$ - is the signal carrier frequency, and $\Delta x_n$ is the range difference in respect to $X_0$.

The inverse Fourier transform of the signal $s_c'(x, k_y)$ along the azimuth dimension is the result of algorithm.

## VI. COMPARISON OF THE ALGORITHMS

The presented algorithms differ in the operating principle because they are based on different properties of the SAR system. During the design of such system, the execution time of the image formulation algorithm and the quality of the obtained images are taken into account.

To verify the first characteristic, the computational complexity of the algorithms in the implemented configurations has been estimated. The number of arithmetic operations (multiplication and summation), extraction of roots and determination of the trigonometric functions values were distinguished. It was assumed that multiplication as well as summation operations take similar amounts of time in arithmetic-logic units, thus those operations are grouped together. Execution time of the remaining operations is dependent on the used calculation algorithms and the argument value, so only the number of their operations could be given but no actual time of their performance. Table I presents a collective

TABLE I
COMPUTATIONAL COMPLEXITY OF THE IMPLEMENTED ALGORITHMS

|  | TDC | RDA | RMA |
|---|---|---|---|
| Arithmetic operations | $NM(37N_a - 2) + 11$ | $\frac{9}{2}NM \log_2 M + M(14N + 8) + \\ + 2N_a(N + 2) + 4N + 23$ | $\frac{3}{2}M(2N + 1)\log_2 M + N(19M + 2) \\ + 3N_a + 24$ |
| Roots extractions | $N_a NM$ | $M + N_a N$ | - |
| Trigonometric functions | $2N_a NM$ | $2N_a N + 1$ | $2NM$ |

list of the obtained results. The given equations determine the number of operations necessary to obtain the image with the dimensions $M \times N$ ($M$ is the number of sounding periods, $N$ is the number of range samples) for a given length of the synthetic aperture $N_a$.

A graphic presentation of a number of arithmetic operations in dependence on number of sounding periods $M$, assuming $N = 1024$ and $N_a = 500$, is shown in Fig. 3. As it can be seen, the computational complexity of the TDC algorithm is many times higher than the RDA and RMA. Thus, it cannot be used for applications that require fast signal processing. The RMA has proven to be little faster than the RDA, and the time of its operation is significantly less dependent on the synthetic aperture length (Fig. 4). However, it should be underlined that the used applications have some simplifications ensuring faster calculations. In consequence, the proportions of computational complexity of RMA and RDA differ from these presented in the literature (e.g. [8]) but the difference in the number of operations is relatively small.
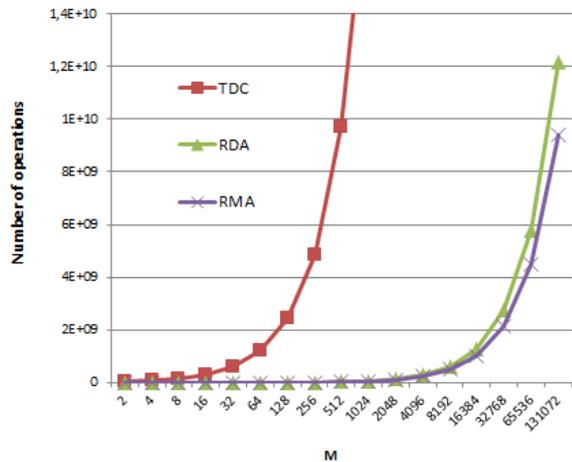


Fig. 3. Number of arithmetic operations in dependence on the number of sounding periods $M$
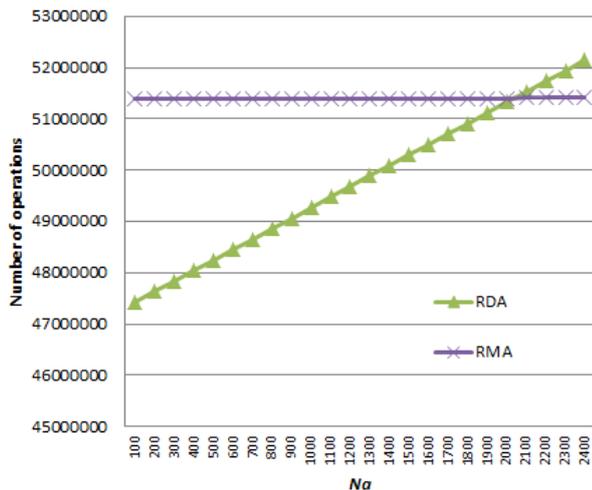


Fig. 4. Number of arithmetic operations in dependence on the length of the synthetic aperture $N_a$

In some SAR systems the quality of the obtained images is much more important than the computation speed. To compare the image quality, the tested algorithms used the same raw SAR signal. The selected fragment of the radar image, presenting the object consisting of 9 reflecting points, arranged in an arrow shape, is shown in Fig. 5.
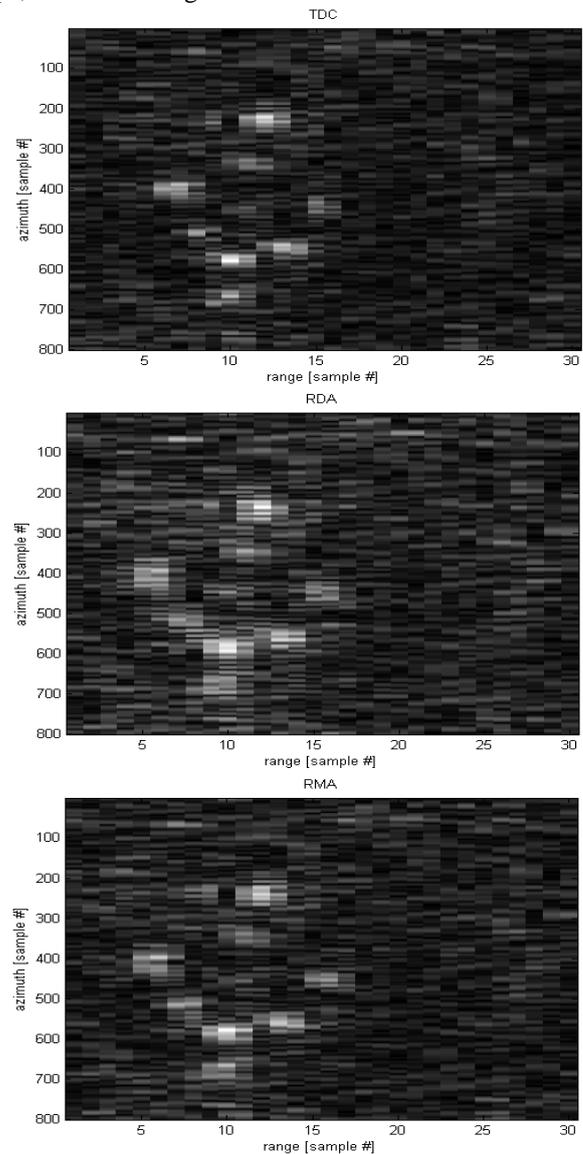


Fig. 5. Radar images obtained by TDC, RDA, and RMA

The seemingly darkest image testifies to the highest contrast and the lowest background noise. This means that more signal energy is focused in the point corresponding to the target position. Small surface of the object on the image also testifies to good algorithm quality. According to that, the best one is TDC algorithm and next RMA and RDA ones.

For additional comparison of the quality of the images, the cross-sections through the point-like target echo at the azimuth coordinate $m = 578$ and the range coordinate $n = 10$ are shown in one diagram (Fig. 6).
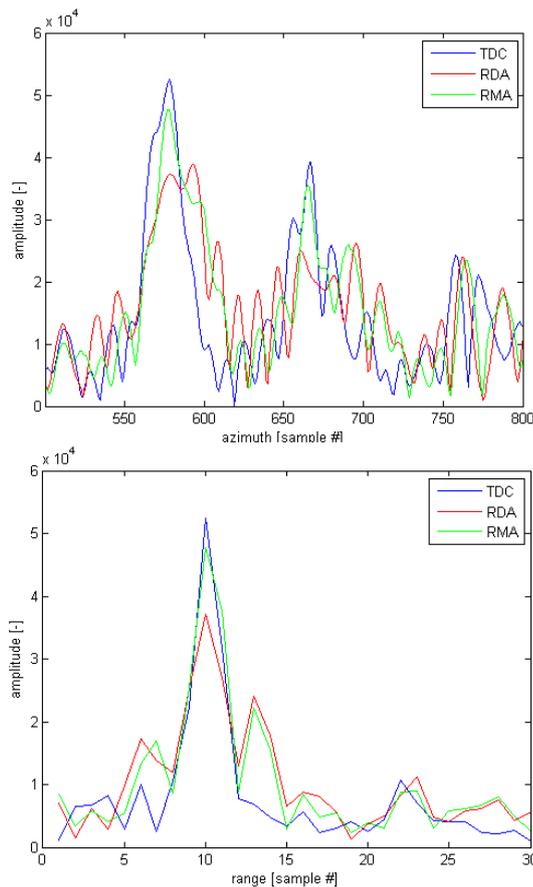
Fig. 6. Azimuth and range cross-sections through selected point ( $m = 578$ , $n = 10$ ) of the radar image

The presented cross-sections confirm the earlier determined qualitative ranking of the algorithms. TDC algorithm ensures the narrowest width of the main lobe and the highest amplitude for the object, the next, in this respect, is the RMA and the most blurred images with relatively high level of side lobes are generated with the RDA. As it was mentioned earlier the RDA is based on approximation of the reference function and it accepts a little poorer image quality which is confirmed by the obtained results.

## VII. Summary

The paper presents an analysis of three SAR image synthesis algorithms: the time domain algorithm TDC and two frequency domain algorithms RDA and RMA, applied for SAR systems operating with FMCW. Their computational complexity, taking into account all modifications and simplifications used for the implemented algorithms, has been theoretically estimated. Also quality of the images obtained by them has been compared.

Having in view the described criteria, in order to obtain an image with the highest quality in applications which do not require fast results, the best choice will be the TDC algorithm. In case of the spectrum algorithms, the better one seems to be the RMA that ensures good-quality results in relatively short time.

## References

[1] J. J. M. de Wit, A. Meta and P. Hoogeboom, "Modified Range-Doppler processing for FM-CW synthetic aperture radar", *IEEE Geoscence and. Remote Sening Letters*, vol. 3, no. 1 , pp.83-87 (2006), DOI: 10.1109/LGRS.2005.856700

[2] M. A. Richards, "Fundamentals of Radar Signal Processing", pp. 385, McGraw-Hill, New York, 2005.

[3] C. Leśnik and A. Kawalec, "Modification of a weighting function for NLFM radar signal designing", *Acta Physica Polonica. A*, vol. 114 No. 6-A (2008), pp. A-143 - A-1479., DOI: 10.12693/APhysPolA.114.A-143

[4] A. Kawalec, C. Ziółkowski, C. Leśnik and J. Pietrasiński, "The Radar Ambiguity Function Application for the Frequency Modulated Signals Designing",. *Acta Physica Polonica. A*, vol. 116 (2009), No. 3, pp. 335 – 339., DOI : 10.12693/APhysPolA.116.335

[5] A. Ribalta, "Time Domain Reconstruction Algorithms for FMCW-SAR", *IEEE Geoscence and. Remote Sening Letters*, vol. 8, no. 3, May 2011, pp. 396-400., DOI: 10.1109/LGRS.2010.2078486

[6] R. Wang, O. Loffeld, H. Nies, S. Knedlik et al., "Focus FMCW SAR data using the wavenumber domain algorithm", *IEEE Transaction on Geoscience and Remote Sensing*, vol. 48, no. 4 (2010), pp.2109-2118, DOI: 10.1109/TGRS.2009.2034368

[7] G. Xue, J. Yang and P. Liu, "Modified range migration algorithm integrated with motion compensation for FMCW SAR", *IET International Radar Conference 2013*, 14-16 April 2013, DOI: 10.1049/cp.2013.0191

[8] I. Cumming and F. H. Wong, "Digital processing of synthetic aperture radar data: algorithms and implementation", pp. 323-361, Artech House Publishers, London, 2005.

[9] R. Bamler, "A comparison of range-doppler and wavenumber domain SAR focusing algorithms", *IEEE Transaction on Geoscience and Remote Sensing*, vol. 30, no. 4 (1992), pp. 706-713, DOI: 10.1109/36.158864

[10] C. Leśnik and P. Serafin, "Design and application of SAR image formulation algorithms with improved quality for data analysis station", Internal technical report of the Institute of Radioelectronics MUT, Warsaw, October 2014, [in Polish].

[11] H.-C. Zeng, J. Chen, W. Liu and W. Yang, "Modified Omega-k algorithm for high-speed platform highly-squint staggered SAR based on azimuth non-uniform interpolation", *Sensors*, vol. 15 (2015), pp. 3750-3765, DOI: 10.3390/s150203750

[12] C. Leśnik, P. Serafin and A. Kawalec, "Azimuth ambiguity suppression in SAR Images using doppler-sensitive signals". *Bulletin of the Polish Academy of Sciences: Techical Sciences*, vol. 63 (2015), pp. 221-227, DOI: 10.1515/bpasts-2015-0026

[13] C. Leśnik, P. Serafin and H. Milczarek, "Experimental verification of the Range-Doppler Algorithm in a continuous wave SAR system", *Przegląd Elektrotechniczny*, R. 91 NR 3/2015 (2015) [in Polish], DOI:10.15199/48.2015.03.26

[14] B.-C. Wang, "Digital signal processing techniques and applications in radar image processing", Wiley, 2008, pp. 226-333.

[15] L. Guo, M. Xing, Y. Tang and J. Dan, "A novel modified Omega-k algorithm for synthetic aperture imaging lidar through the atmosphere", *Sensors*, vol. 8 (2008), pp. 3056-3066, DOI: 10.3390/s8053056